

RESEARCH PAPER

Quantum Dots Gold Nanoparticle /Porous Silicon/Silicon for Solar Cell Applications

M.J. Khalifa¹, Muneer H Jadaua¹, Ahmed N. Abd^{2,*}

¹ Department of Physics, College of Science, Wasit University, Iraq

² Department of Physics, College of Science, Mustansiriyah University, Baghdad, Iraq

ARTICLE INFO

Article History:

Received 10 July 2020

Accepted 19 September 2020

Published 01 December 2020

Keywords:

I-V characteristics

Gold Nanoparticles

Porous silicon (PS)

Solar cell

SPR in metal NPs

ABSTRACT

Gold nanoparticles (AuNPs) were synthesized by electrolysis method as colloidal nanoparticles and deposited on both glass substrates and p-type porous silicon (PSi) to prepare films by using drop casting method to improve the performance of PS/Si solar cell. PS was prepared by electrochemical etching process (ECE) for p-Si wafers. The optical properties of PS and AuNPs were examined. The structural and morphological properties for PSi and gold nanostructure (AuNSs) deposited on glass substrate have been studied by using (XRD) and Atomic Force Microscope (AFM) respectively. TEM testing for AuNPs was investigated. XRD pattern of PSi showed that it had single crystalline structure, whereas for Au nanostructure it was polycrystalline one. AFM confirmed the nanometric size of both AuNSs and PSi it was around 40 nm for AuNSs and 62 nm for PS. The AuNPs diffusion effect on the electrical properties of PS/Si heterojunction was studied. The photovoltaic characteristics of AuNPs/PS/Si/Al Solar cell were reported and the efficiency of solar cell was 15.67% and F.F is 34.31%.

How to cite this article

Khalifa M.J., H Jadaua M., Ahmed N. Quantum Dots Gold Nanoparticle /Porous Silicon/Silicon for Solar Cell Applications. J Nanostruct, 2020; 10(4): 863-870. DOI: 10.22052/JNS.2020.04.019

INTRODUCTION

Solar energy conversion is attractive because it is both inexhaustible and pollution-free [1]. On the other hand, nanoparticles have received great attention due to their unique chemical and physical properties in the past decades, which differ from those of bulk materials or single atoms [2]. The unique electronic and chemical properties of metallic nanoparticles have attracted the attention of physicists, chemists, biologists and engineers who want to use them to develop a new generation of nanoscale devices. Metallic nanoparticles such as gold and silver exhibit remarkable photocatalytic activity under visible UV rays as evidenced by the fusion and fragmentation process resulting from photocatalysis [3]

, They used for many applications in, photonics,

biosensing, intracellular, gene regulation and catalysis [4–8]. Porous silicon (PS) can be considered as a silicon crystal having a network of voids in it. The nanosized voids in the silicon bulk result in a sponge-like structure of pores and channels surrounded with a skeleton of crystalline silicon nanowires [9]. Due to the powerful room temperature visible photoluminescence, PS has drawn a lot of interest which was first observed by Canham in 1990[10]. PS has a number of unique properties such as visible light emission and enhanced light absorption. Electrochemical anodization and stain etching are remaining the most common methods for PS substrate fabrication, which enable the production of PS with tailored morphological properties (porosity, pore size, and depth of pores). Coupling system

* Corresponding Author Email:

ahmed_naji_abd@uomustansiriyah.edu.iq

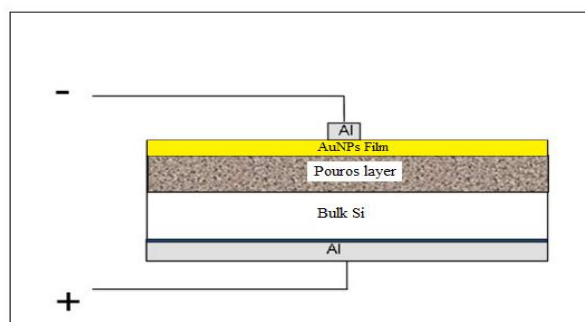


Fig. 1. image of AuNPs/PS/p-Si solar cell

consisting of metal nanoparticles (NPs) and semiconductor nanocrystals (NCs) has been subject of great interest for scientific communities [11]. The surface Plasmon resonance in metal nanoparticles causes the interaction between the NPs and NCs can modify spectral feature of semiconductor NCs to enhance the emission efficiency because it involved charge transfer across the semiconductor/metal interface [12].

MATERIALS AND METHODS

Gold nanoparticles (Au NPs) prepared by electrolysis cell. The electrodes of this cell consist of a Mo plate as a negative electrode and Au layer as a positive electrode, and the dimensions of both layers (3, 2 and 0.2) cm in length, width and thick respectively. The anode of this cell connected in series DC voltage (5 volts). 80(water):10(HCl) was used as an electrolyte liquid and the reaction time was about 30 minutes. The drop casting method was used to deposit colloidal Au NPs on glass substrate (2x2) cm² to prepare thin films. In an ultrasonic bath, these substrates are washed with alcohol to eliminate impurities and residuals from their surface. In the preparation of the Au thin film on glass substrates, three drops of colloidal Au NPs were used. Same process used to deposit colloidal Au NPs on PS/Si heterojunction to produce Au NPs/PS/p-Si solar cell as shown in Fig. 1.

The crystalline wafers of p-Si sheets with [resistance of (4 to 20 W.cm), thickness is 508 μm and orientation (100). are used as substrates. The substrate area was (2 × 2) cm². Electrochemical etching was performed at (1:1) HF (48%): ethanol (99.99) mixture at room temperature using gold electrode. Current density (J) =10mA/cm² was applied for 15 minutes to produce an etched circular area around(0.785cm²).X-ray diffraction

pattern of Au NPs and PSi were measured by (SHIMADZU, XRD-6000) using CuKα radiation line of wavelength of 1.54 Å in 2θ ranging from 20° to 80°. Transmittance and OPTIMA, SP 3000 UV-VIS. TEM study has been carried out by ZEISS-EM10C-100kV, for colloidal Au NPS. AFM (AA 3000 Scanning Probe Microscope) was used to study the morphology of the prepared Au NPs and PSi samples to determine the particles dimensions range and their statistical distributions. I-V measurements tools are: digital Keithly-616 electrometer, Tektronics CDM 250 multimeter and a 0 to 10V dual Farnel LT30/2 power supply were used.

RESULTS AND DISCUSSION

XRD of the Au NPs and p-type PSi were tested by Kα Cu source line of 1.543 Å wavelength as mentioned above. XRD patterns of p-type PSi and AuNPs are shown in Fig. 2 and Fig. 3 respectively. Fig. 2 shows the XRD pattern of p-type PS layer which show single crystalline structure of this material, but it has significant peak broadening corresponding to the diffraction angle (69.28°), which is interpreted as nanocrystalline size effect.

Fig. 3 Shows XRD pattern of Au nanostructures (Au NSs) deposited on glass substrate. The XRD pattern contains three main peaks at 2θ=38.12°,44.3°and 64.6° all three peaks corresponding to standard Bragg reflections (111), (200) and (220) of face center cubic lattice. The broadening of the stronger peak at angle 38.1294° which give evidence of formation the nanostructure. The sharp peaks are match with the standard peaks of gold (JCPDS file:04-0784). The multi-peaks in the XRD pattern of Au NSs which indicated that the material had the polycrystalline structure.

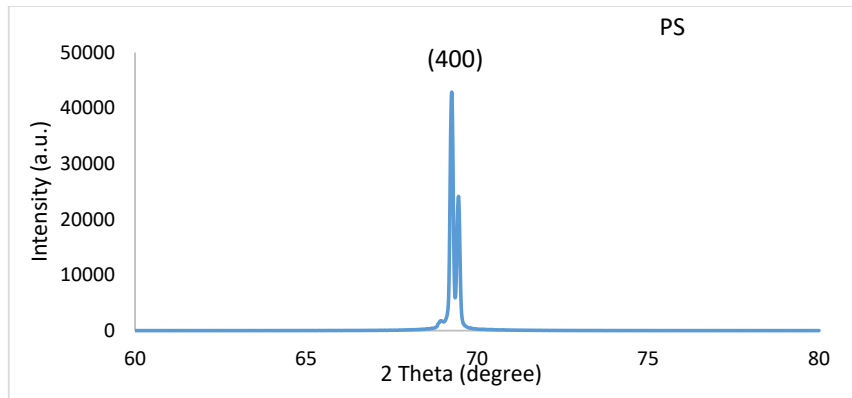


Fig. 2. XRD pattern of p-type PS

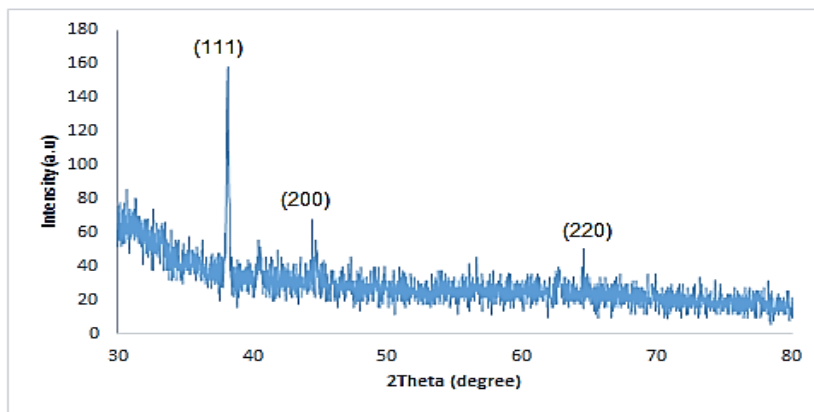


Fig. 3. The XRD pattern of Au NPs

Table 1. The values of the grain size, FWHM, the strain(δ) and the dislocating density η of gold nanoparticles as a film and p-type PS.

Material	2Theta (Deg)	β (deg)	D_s (nm)	$\delta * 10^{14}$ lines/m ²	$\eta * 10^{-3}$
Gold	38.1294	0.1327	67.5	2.194	0.5471
PS	69.2805	0.11	91	1.207	0.3973

By using the width of a sharp peak appears at the angle 38.12° on 2θ scale in Scherer law [13]:

$$D_s = \frac{K\lambda}{\beta \cos\theta} \tag{1}$$

where D_s is the grain size, k represents shape factor, θ is Brag angle and (β) represents [the full width at half maximum (FWHM)] in degrees, the size of the formed Au NPs was (67.5nm). Microstrain value (d) and the dislocating density (η) values measured with the use of the relationships in equations (2) and (3) [14]:

$$\eta = \frac{\beta \cos\theta}{4} \text{ (lin}^{-2}\text{m}^{-4}\text{)} \tag{2}$$

$$\delta = 1/D^2 \text{ (lines/m}^2\text{)} \tag{3}$$

By applying the same relations which mention above on porous silicon, which has broadening peak at the diffraction angle (69.2805 °), we get that the grain size of PS is about 90 nm.

The optical energy gap of Au NPs has been calculated from its transmittance, Fig. 4 appears the transmission as verses of the λ of the colloidal Au NPs which prepare by electrolysis process. On this figure, it can be observed that minimum transmittance at wavelength 315nm, then sharp increasing to the wavelength 450nm.the maximum transmittance be in the region from 450nm to 900 nm and it be stable. This behavior means that the

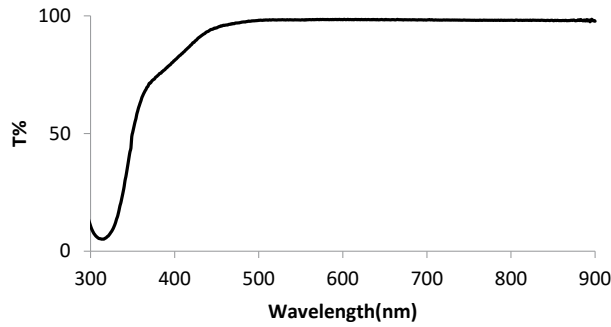


Fig. 4. The transmittance spectrum of AuNPs

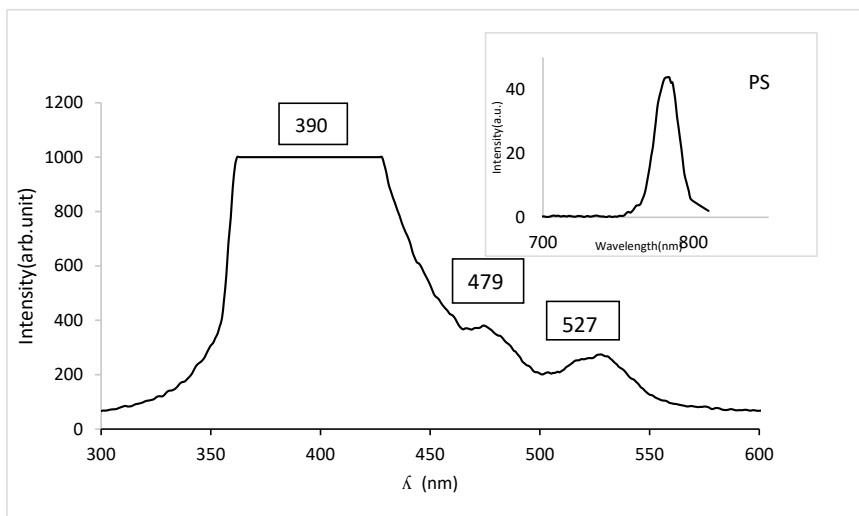


Fig. 5. absorption spectrum of Au NPs and PS

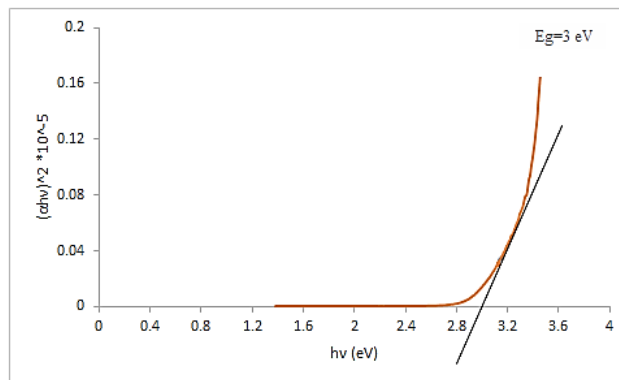


Fig. 6. $(\alpha hv)^2$ versus optical energy gap of Au NPs

material has high absorbance at UV region so it be effective, but in the region of 372 nm (the Au NPs material behaves as a window).

The photoluminescence(PL) spectrum of Au

NPs in Fig. 6 shows a peak at 527nm which can be indicated to the local surface Plasmon resonance band of Au NPs. PL spectrum have other different peak positions at 479nm and 390nm may be

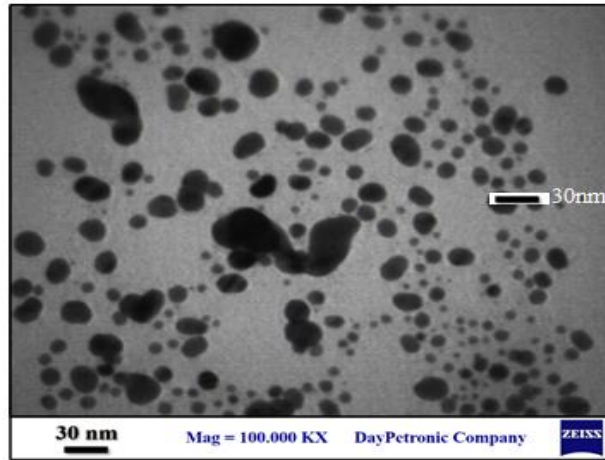


Fig. 7. TEM image of a colloidal AuNPs.

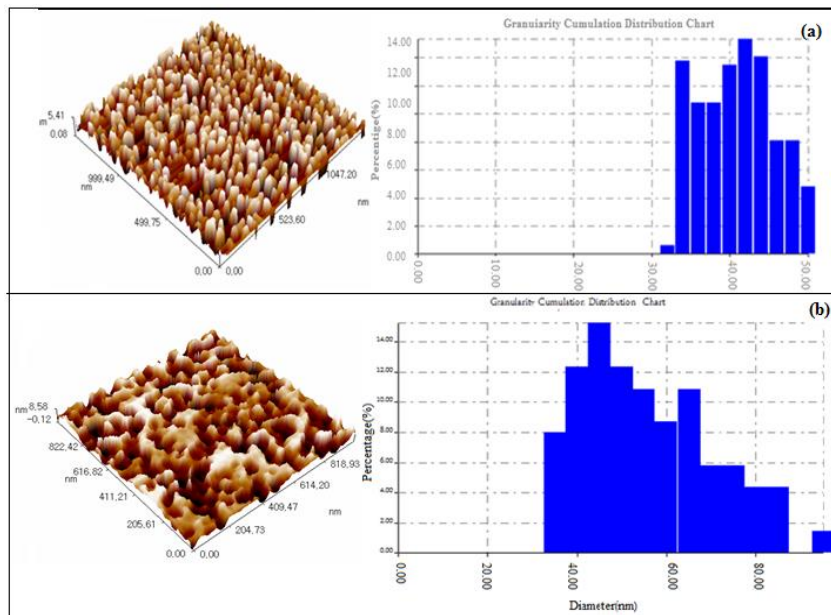


Fig. 8. AFM image and Granularity Cumulation distribution Chart of (a)Au NPs and (b)PS

attributed to formation of AuNPs in different sizes, and this result agree with others[15].While the inset figure shows the PL spectrum of PS , it characterized by the presence of one sharp peak in red band region(780nm) which refers to the fundamental absorption of PS.

Fig. 6 shows the optical energy band gap (E_g) of Au NPs calculated from the plot of $(\alpha hu)^2$ vs. (hu) where (α) is the absorption coefficient, which is found to be (3 eV) by extrapolating the linear portion of the curve toward the photon energy axis).

Transmission electron microscope (TEM)

image for colloidal Au NPs is shown in Fig. 7. The TEM micro image confirms the formation of Au NPs having the diameter ranging from (5-30) nm. The gold image in TEM is represented by the dark, small and ball shape particle.

The morphology of PS surface and Au nanostructure surfaces were studied by the AFM images as shown in Fig. 8(a, b). It is shown smooth and homogeneous structures for both samples. The average size of the grain was evaluated from AFM analyzing with the use software and it has been found to be around 54nm and 40 nm for PS and Au NSs respectively.

Table 2. values of Avg. Diameter, Roughens average and Root mean square of Au NPs and PS

Material	Avg. Diameter (nm)	Roughens average (nm)	Root mean square (nm)
Au NPS	39.93	1.33	1.54
PS	53.79	2.19	2.53

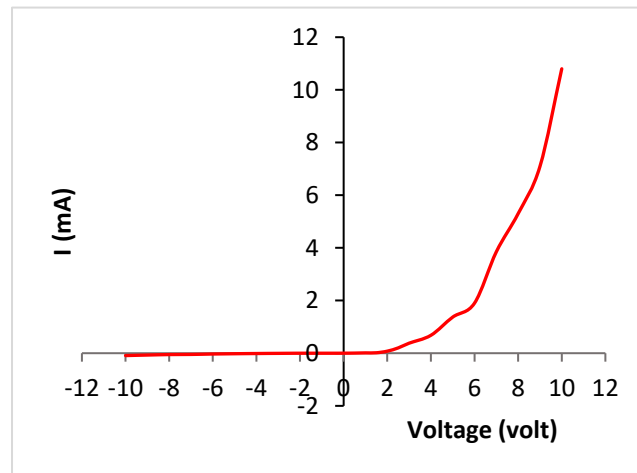


Fig. 9. Dark (I-V) of the Au NPs/PS/p-Si heterojunction

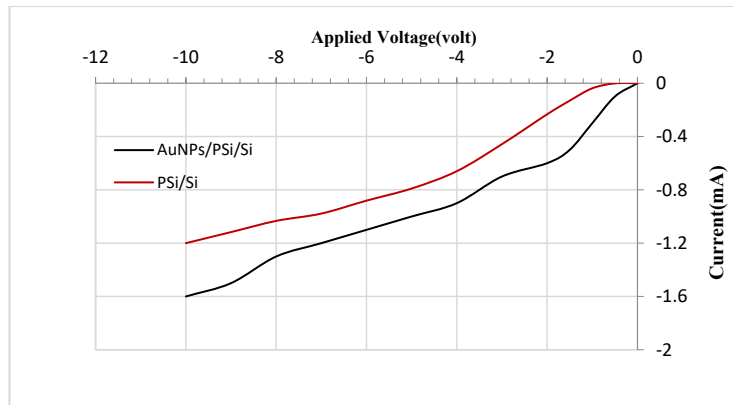


Fig. 10. Illuminated I-V characteristic of the Au NPs/PS/Si heterojunction

Table 2 illustrates the results of AFM study of Au nanostructure as thin film on glass substrate and p-type PS.

The (I-V) characterization commonly used as characterization tool for the devices. The (I) t is measured as a function of voltage of the heterojunction in both cases (dark and light). The dark I-V properties in inverse and forward directions of Au/PS/Si are shown in Fig. 9. The forward current of heterojunction is limited at

voltage less than 2 volt. It is generated by the following majority carriers when the applied voltage injects these carriers which lead to decrease the width of the depletion layer. In this region the diffusion current which is dominated.

Whereas Fig. 10 represents the (I-V) of Au NSs/PS/p-Si heterojunction under illumination, it shows that the Reverse photocurrent as a function of bias voltage, photocurrent increases with reverse bias voltage after add Au NPs and no

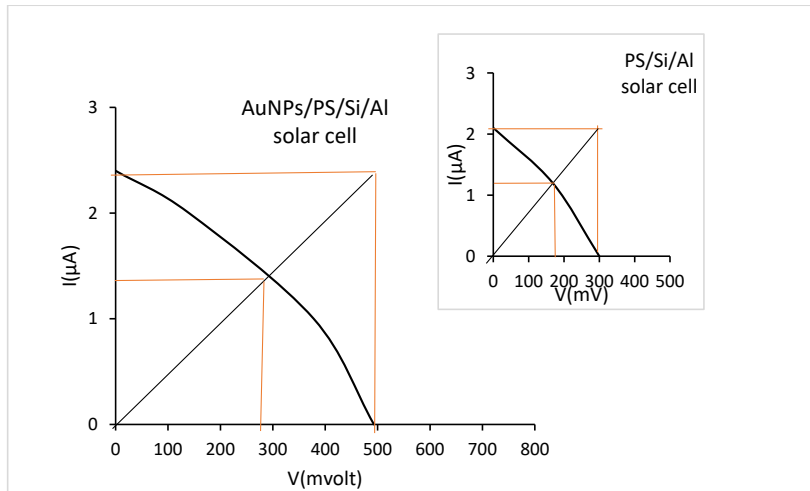


Fig. 11. I-V curve of porous silicon solar cell with and without gold nanoparticles (the inset figure is the PSi/Si solar cell without AuNPs)

Table 3. I-V measurements of PS/Si solar cells with and without Au NPs

Material	Avg. Diameter (nm)	Roughness average (nm)	Root mean square (nm)
Au NPS	39.93	1.33	1.54
PS	53.79	2.19	2.53

saturation region was observed.

Fig. 11 represent the optoelectronic properties of Au/PSi/Si solar cell and the inset figure show the optoelectronic properties for PSi/Si solar cell. Open circuit voltage (V_{oc} , $R=\infty$, $I=0$) the increasing in (I_{sc}) and (V_{oc}), Resulting in an increasing output power. This leads to increasing efficiency of solar cells. The efficiency of solar cell ($\eta\%$) is a ratio of = p_m / p_{in} 100% and full factor (F.F)= $(I_m V_m / I_{sc} V_{oc})$ 100% .The photovoltaic parameters of Au NPs/PS/p-Si solar cell and standard PS/p-Si solar cell are given in Table 3.

CONCLUSION

Gold nanoparticles (prepared by electrolysis method) was added into PSi/Si solar cell to enhance the photovoltaic parameters. Effect of localized SPR of Au NPs can be enhancing the efficiency of solar cell by increasing the light absorption ability. Then, increasing the photocurrent. Drop casting method was used to prepare thin film of Au NPs on PSi layer. After adding Au NPs, the efficiency increased from (7.78% to 15.67) and F.F also increased from (32% to 34.31) because of increasing the photocurrent. PS was successfully

prepare using electrochemical etching of p-Si wafers. Au NPs shows good transparency in the spectral range 430nm 900 nm. Au NPs consider effective material at the UV region so it could be act as a detector in this region.

CONFLICT OF INTEREST

The authors declare that there is no conflict of interests regarding the publication of this manuscript.

REFERENCES

1. ISLAM S. S. Semiconductor Physics and Devices. OXFORD UNIVERSITY PRESS, Oxford. 2005: 455.
2. Jabbar AH. Fabrication and Characterization of CuO:NiO Composite for Solar Cell Applications. Journal of Advanced Research in Dynamical and Control Systems. 2020;24(4):179-86.
3. Kamat PV. Photophysical, Photochemical and Photocatalytic Aspects of Metal Nanoparticles. The Journal of Physical Chemistry B. 2002;106(32):7729-44.
4. Abd AN, Habubi NE, Ismail RA. Preparation of colloidal cadmium selenide nanoparticles by pulsed laser ablation in methanol and toluene. Journal of Materials Science: Materials in Electronics. 2014;25(7):3190-4.
5. Rosi NL. Oligonucleotide-Modified Gold Nanoparticles for Intracellular Gene Regulation. Science.

- 2006;312(5776):1027-30.
6. Hyunwoo L, Eunjoo L, Soohong L. Investigation of nanoporous silicon antireflection coatings for crystalline silicon solar cells. 2006 IEEE Nanotechnology Materials and Devices Conference; 2006/10: IEEE; 2006.
 7. Millstone JE, Hurst SJ, Métraux GS, Cutler JI, Mirkin CA. Colloidal Gold and Silver Triangular Nanoprisms. *Small*. 2009;5(6):646-64.
 8. Wang C, Hu Y, Lieber CM, Sun S. Ultrathin Au Nanowires and Their Transport Properties. *Journal of the American Chemical Society*. 2008;130(28):8902-3.
 9. Ahmed N. Abd, Nadir F. Habubi, Ali H. Reshak and Hazim L. Mansour, Enhancing the Electrical Properties of Porous Silicon Photodetector by Depositing MWCNTs. *International Journal of Nano electronics and Materials*. 2018; 11(3): 241-248.
 10. Nagham Abdulameer Yasir, Alzubaidy Muneer Hlail and Ali Kamel Mohsin, Characterization of Titania Thin Film Behavior Preparation by Spray Pyrolysis. *Indian Journal of Natural Sciences*. 2018; 9(51); 15700-15709.
 11. Patterson AL. The Scherrer Formula for X-Ray Particle Size Determination. *Physical Review*. 1939;56(10):978-82.
 12. Yang S, Cai W, Zhang H, Xu X, Zeng H. Size and Structure Control of Si Nanoparticles by Laser Ablation in Different Liquid Media and Further Centrifugation Classification. *The Journal of Physical Chemistry C*. 2009;113(44):19091-5.
 13. Chen GX, Hong MH, Lan B, Wang ZB, Lu YF, Chong TC. A convenient way to prepare magnetic colloids by direct Nd:YAG laser ablation. *Applied Surface Science*. 2004;228(1-4):169-75.
 14. Smestad G, Kunst M, Vial C. Photovoltaic response in electrochemically prepared photoluminescent porous silicon. *Solar Energy Materials and Solar Cells*. 1992;26(4):277-83.
 15. Amran TST, Hashim MR, Al-Obaidi NKA, Yazid H, Adnan R. Optical absorption and photoluminescence studies of gold nanoparticles deposited on porous silicon. *Nanoscale Research Letters*. 2013;8(1):35.